

# Observation of Radiative Decay $D^0 \rightarrow \phi\gamma$

K. Abe,<sup>9</sup> K. Abe,<sup>44</sup> N. Abe,<sup>47</sup> R. Abe,<sup>30</sup> T. Abe,<sup>9</sup> I. Adachi,<sup>9</sup> Byoung Sup Ahn,<sup>16</sup> H. Aihara,<sup>46</sup> M. Akatsu,<sup>23</sup> M. Asai,<sup>10</sup> Y. Asano,<sup>51</sup> T. Aso,<sup>50</sup> V. Aulchenko,<sup>2</sup> T. Aushev,<sup>13</sup> S. Bahinipati,<sup>5</sup> A. M. Bakich,<sup>41</sup> Y. Ban,<sup>34</sup> E. Banas,<sup>28</sup> S. Banerjee,<sup>42</sup> A. Bay,<sup>19</sup> I. Bedny,<sup>2</sup> P. K. Behera,<sup>52</sup> I. Bizjak,<sup>14</sup> A. Bondar,<sup>2</sup> A. Bozek,<sup>28</sup> M. Bračko,<sup>21,14</sup> J. Brodzicka,<sup>28</sup> T. E. Browder,<sup>8</sup> M.-C. Chang,<sup>27</sup> P. Chang,<sup>27</sup> Y. Chao,<sup>27</sup> K.-F. Chen,<sup>27</sup> B. G. Cheon,<sup>40</sup> R. Chistov,<sup>13</sup> S.-K. Choi,<sup>7</sup> Y. Choi,<sup>40</sup> M. Danilov,<sup>13</sup> M. Dash,<sup>53</sup> E. A. Dodson,<sup>8</sup> L. Y. Dong,<sup>11</sup> R. Dowd,<sup>22</sup> J. Dragic,<sup>22</sup> A. Drutskoy,<sup>13</sup> S. Eidelman,<sup>2</sup> V. Eiges,<sup>13</sup> Y. Enari,<sup>23</sup> D. Epifanov,<sup>2</sup> C. W. Everton,<sup>22</sup> F. Fang,<sup>8</sup> H. Fujii,<sup>9</sup> C. Fukunaga,<sup>48</sup> N. Gabyshev,<sup>9</sup> A. Garmash,<sup>2,9</sup> T. Gershon,<sup>9</sup> G. Gokhroo,<sup>42</sup> B. Golob,<sup>20,14</sup> A. Gordon,<sup>22</sup> M. Grosse Perdekamp,<sup>36</sup> H. Guler,<sup>8</sup> R. Guo,<sup>25</sup> J. Haba,<sup>9</sup> C. Hagner,<sup>53</sup> F. Handa,<sup>45</sup> K. Hara,<sup>32</sup> T. Hara,<sup>32</sup> Y. Harada,<sup>30</sup> N. C. Hastings,<sup>9</sup> K. Hasuko,<sup>36</sup> H. Hayashii,<sup>24</sup> M. Hazumi,<sup>9</sup> E. M. Heenan,<sup>22</sup> I. Higuchi,<sup>45</sup> T. Higuchi,<sup>9</sup> L. Hinz,<sup>19</sup> T. Hojo,<sup>32</sup> T. Hokuue,<sup>23</sup> Y. Hoshi,<sup>44</sup> K. Hoshina,<sup>49</sup> W.-S. Hou,<sup>27</sup> Y. B. Hsiung,<sup>27</sup> H.-C. Huang,<sup>27</sup> T. Igaki,<sup>23</sup> Y. Igarashi,<sup>9</sup> T. Iijima,<sup>23</sup> K. Inami,<sup>23</sup> A. Ishikawa,<sup>23</sup> H. Ishino,<sup>47</sup> R. Itoh,<sup>9</sup> M. Iwamoto,<sup>3</sup> H. Iwasaki,<sup>9</sup> M. Iwasaki,<sup>46</sup> Y. Iwasaki,<sup>9</sup> H. K. Jang,<sup>39</sup> R. Kagan,<sup>13</sup> H. Kakuno,<sup>47</sup> J. Kaneko,<sup>47</sup> J. H. Kang,<sup>55</sup> J. S. Kang,<sup>16</sup> P. Kapusta,<sup>28</sup> M. Kataoka,<sup>24</sup> S. U. Kataoka,<sup>24</sup> N. Katayama,<sup>9</sup> H. Kawai,<sup>3</sup> H. Kawai,<sup>46</sup> Y. Kawakami,<sup>23</sup> N. Kawamura,<sup>1</sup> T. Kawasaki,<sup>30</sup> N. Kent,<sup>8</sup> A. Kibayashi,<sup>47</sup> H. Kichimi,<sup>9</sup> D. W. Kim,<sup>40</sup> Heejong Kim,<sup>55</sup> H. J. Kim,<sup>55</sup> H. O. Kim,<sup>40</sup> Hyunwoo Kim,<sup>16</sup> J. H. Kim,<sup>40</sup> S. K. Kim,<sup>39</sup> T. H. Kim,<sup>55</sup> K. Kinoshita,<sup>5</sup> S. Kobayashi,<sup>37</sup> P. Koppenburg,<sup>9</sup> K. Korotushenko,<sup>35</sup> S. Korpar,<sup>21,14</sup> P. Križan,<sup>20,14</sup> P. Krokovny,<sup>2</sup> R. Kulasiri,<sup>5</sup> S. Kumar,<sup>33</sup> E. Kurihara,<sup>3</sup> A. Kusaka,<sup>46</sup> A. Kuzmin,<sup>2</sup> Y.-J. Kwon,<sup>55</sup> J. S. Lange,<sup>6,36</sup> G. Leder,<sup>12</sup> S. H. Lee,<sup>39</sup> T. Lesiak,<sup>28</sup> J. Li,<sup>38</sup> A. Limosani,<sup>22</sup> S.-W. Lin,<sup>27</sup> D. Liventsev,<sup>13</sup> R.-S. Lu,<sup>27</sup> J. MacNaughton,<sup>12</sup> G. Majumder,<sup>42</sup> F. Mandl,<sup>12</sup> D. Marlow,<sup>35</sup> T. Matsubara,<sup>46</sup> T. Matsuishi,<sup>23</sup> H. Matsumoto,<sup>30</sup> S. Matsumoto,<sup>4</sup> T. Matsumoto,<sup>48</sup> A. Matyja,<sup>28</sup> Y. Mikami,<sup>45</sup> W. Mitaroff,<sup>12</sup> K. Miyabayashi,<sup>24</sup> Y. Miyabayashi,<sup>23</sup> H. Miyake,<sup>32</sup> H. Miyata,<sup>30</sup> L. C. Moffitt,<sup>22</sup> D. Mohapatra,<sup>53</sup> G. R. Moloney,<sup>22</sup> G. F. Moorhead,<sup>22</sup> S. Mori,<sup>51</sup> T. Mori,<sup>47</sup> J. Mueller,<sup>9</sup> A. Murakami,<sup>37</sup> T. Nagamine,<sup>45</sup> Y. Nagasaka,<sup>10</sup> T. Nakadaira,<sup>46</sup> E. Nakano,<sup>31</sup> M. Nakao,<sup>9</sup> H. Nakazawa,<sup>9</sup> J. W. Nam,<sup>40</sup> S. Narita,<sup>45</sup> Z. Natkaniec,<sup>28</sup> K. Neichi,<sup>44</sup> S. Nishida,<sup>9</sup> O. Nitoh,<sup>49</sup> S. Noguchi,<sup>24</sup> T. Nozaki,<sup>9</sup> A. Ogawa,<sup>36</sup> S. Ogawa,<sup>43</sup> F. Ohno,<sup>47</sup> T. Ohshima,<sup>23</sup> T. Okabe,<sup>23</sup> S. Okuno,<sup>15</sup> S. L. Olsen,<sup>8</sup> Y. Onuki,<sup>30</sup> W. Ostrowicz,<sup>28</sup> H. Ozaki,<sup>9</sup> P. Pakhlov,<sup>13</sup> H. Palka,<sup>28</sup> C. W. Park,<sup>16</sup> H. Park,<sup>18</sup> K. S. Park,<sup>40</sup> N. Parslow,<sup>41</sup> L. S. Peak,<sup>41</sup> M. Pernicka,<sup>12</sup> J.-P. Perroud,<sup>19</sup> M. Peters,<sup>8</sup> L. E. Piilonen,<sup>53</sup> F. J. Ronga,<sup>19</sup> N. Root,<sup>2</sup> M. Rozanska,<sup>28</sup> H. Sagawa,<sup>9</sup> S. Saitoh,<sup>9</sup> Y. Sakai,<sup>9</sup> H. Sakamoto,<sup>17</sup> H. Sakaue,<sup>31</sup> T. R. Sarangi,<sup>52</sup> M. Satapathy,<sup>52</sup> A. Satpathy,<sup>9,5</sup> O. Schneider,<sup>19</sup> S. Schrenk,<sup>5</sup> J. Schümann,<sup>27</sup> C. Schwanda,<sup>9,12</sup> A. J. Schwartz,<sup>5</sup> T. Seki,<sup>48</sup> S. Semenov,<sup>13</sup> K. Senyo,<sup>23</sup> Y. Settai,<sup>4</sup> R. Seuster,<sup>8</sup> M. E. Sevior,<sup>22</sup> T. Shibata,<sup>30</sup> H. Shibuya,<sup>43</sup> M. Shimoyama,<sup>24</sup> B. Shwartz,<sup>2</sup> V. Sidorov,<sup>2</sup> V. Siegle,<sup>36</sup> J. B. Singh,<sup>33</sup> N. Soni,<sup>33</sup> S. Stanič,<sup>51</sup> M. Starič,<sup>14</sup> A. Sugi,<sup>23</sup> A. Sugiyama,<sup>37</sup> K. Sumisawa,<sup>9</sup> T. Sumiyoshi,<sup>48</sup> K. Suzuki,<sup>9</sup> S. Suzuki,<sup>54</sup> S. Y. Suzuki,<sup>9</sup> S. K. Swain,<sup>8</sup> O. Tajima,<sup>45</sup> K. Takahashi,<sup>47</sup> F. Takasaki,<sup>9</sup> B. Takeshita,<sup>32</sup> K. Tamai,<sup>9</sup> Y. Tamai,<sup>32</sup> N. Tamura,<sup>30</sup> K. Tanabe,<sup>46</sup> J. Tanaka,<sup>46</sup> M. Tanaka,<sup>9</sup> G. N. Taylor,<sup>22</sup> A. Tchouvikov,<sup>35</sup> Y. Teramoto,<sup>31</sup> S. Tokuda,<sup>23</sup> M. Tomoto,<sup>9</sup> T. Tomura,<sup>46</sup> S. N. Tovey,<sup>22</sup>

K. Trabelsi,<sup>8</sup> T. Tsuboyama,<sup>9</sup> T. Tsukamoto,<sup>9</sup> K. Uchida,<sup>8</sup> S. Uehara,<sup>9</sup> K. Ueno,<sup>27</sup>  
T. Uglov,<sup>13</sup> Y. Unno,<sup>3</sup> S. Uno,<sup>9</sup> N. Uozaki,<sup>46</sup> Y. Ushiroda,<sup>9</sup> S. E. Vahsen,<sup>35</sup> G. Varner,<sup>8</sup>  
K. E. Varvell,<sup>41</sup> C. C. Wang,<sup>27</sup> C. H. Wang,<sup>26</sup> J. G. Wang,<sup>53</sup> M.-Z. Wang,<sup>27</sup>  
M. Watanabe,<sup>30</sup> Y. Watanabe,<sup>47</sup> L. Widhalm,<sup>12</sup> E. Won,<sup>16</sup> B. D. Yabsley,<sup>53</sup> Y. Yamada,<sup>9</sup>  
A. Yamaguchi,<sup>45</sup> H. Yamamoto,<sup>45</sup> T. Yamanaka,<sup>32</sup> Y. Yamashita,<sup>29</sup> Y. Yamashita,<sup>46</sup>  
M. Yamauchi,<sup>9</sup> H. Yanai,<sup>30</sup> Heyoung Yang,<sup>39</sup> J. Yashima,<sup>9</sup> P. Yeh,<sup>27</sup> M. Yokoyama,<sup>46</sup>  
K. Yoshida,<sup>23</sup> Y. Yuan,<sup>11</sup> Y. Yusa,<sup>45</sup> H. Yuta,<sup>1</sup> C. C. Zhang,<sup>11</sup> J. Zhang,<sup>51</sup> Z. P. Zhang,<sup>38</sup>  
Y. Zheng,<sup>8</sup> V. Zhilich,<sup>2</sup> Z. M. Zhu,<sup>34</sup> T. Ziegler,<sup>35</sup> D. Žontar,<sup>20,14</sup> and D. Zürcher<sup>19</sup>

(The Belle Collaboration)

<sup>1</sup>*Aomori University, Aomori*

<sup>2</sup>*Budker Institute of Nuclear Physics, Novosibirsk*

<sup>3</sup>*Chiba University, Chiba*

<sup>4</sup>*Chuo University, Tokyo*

<sup>5</sup>*University of Cincinnati, Cincinnati, Ohio 45221*

<sup>6</sup>*University of Frankfurt, Frankfurt*

<sup>7</sup>*Gyeongsang National University, Chinju*

<sup>8</sup>*University of Hawaii, Honolulu, Hawaii 96822*

<sup>9</sup>*High Energy Accelerator Research Organization (KEK), Tsukuba*

<sup>10</sup>*Hiroshima Institute of Technology, Hiroshima*

<sup>11</sup>*Institute of High Energy Physics,*

*Chinese Academy of Sciences, Beijing*

<sup>12</sup>*Institute of High Energy Physics, Vienna*

<sup>13</sup>*Institute for Theoretical and Experimental Physics, Moscow*

<sup>14</sup>*J. Stefan Institute, Ljubljana*

<sup>15</sup>*Kanagawa University, Yokohama*

<sup>16</sup>*Korea University, Seoul*

<sup>17</sup>*Kyoto University, Kyoto*

<sup>18</sup>*Kyungpook National University, Taegu*

<sup>19</sup>*Institut de Physique des Hautes Énergies, Université de Lausanne, Lausanne*

<sup>20</sup>*University of Ljubljana, Ljubljana*

<sup>21</sup>*University of Maribor, Maribor*

<sup>22</sup>*University of Melbourne, Victoria*

<sup>23</sup>*Nagoya University, Nagoya*

<sup>24</sup>*Nara Women's University, Nara*

<sup>25</sup>*National Kaohsiung Normal University, Kaohsiung*

<sup>26</sup>*National Lien-Ho Institute of Technology, Miao Li*

<sup>27</sup>*Department of Physics, National Taiwan University, Taipei*

<sup>28</sup>*H. Niewodniczanski Institute of Nuclear Physics, Krakow*

<sup>29</sup>*Nihon Dental College, Niigata*

<sup>30</sup>*Niigata University, Niigata*

<sup>31</sup>*Osaka City University, Osaka*

<sup>32</sup>*Osaka University, Osaka*

<sup>33</sup>*Panjab University, Chandigarh*

<sup>34</sup>*Peking University, Beijing*

<sup>35</sup>*Princeton University, Princeton, New Jersey 08545*

<sup>36</sup>*RIKEN BNL Research Center, Upton, New York 11973*

<sup>37</sup>*Saga University, Saga*  
<sup>38</sup>*University of Science and Technology of China, Hefei*  
<sup>39</sup>*Seoul National University, Seoul*  
<sup>40</sup>*Sungkyunkwan University, Suwon*  
<sup>41</sup>*University of Sydney, Sydney NSW*  
<sup>42</sup>*Tata Institute of Fundamental Research, Bombay*  
<sup>43</sup>*Toho University, Funabashi*  
<sup>44</sup>*Tohoku Gakuin University, Tagajo*  
<sup>45</sup>*Tohoku University, Sendai*  
<sup>46</sup>*Department of Physics, University of Tokyo, Tokyo*  
<sup>47</sup>*Tokyo Institute of Technology, Tokyo*  
<sup>48</sup>*Tokyo Metropolitan University, Tokyo*  
<sup>49</sup>*Tokyo University of Agriculture and Technology, Tokyo*  
<sup>50</sup>*Toyama National College of Maritime Technology, Toyama*  
<sup>51</sup>*University of Tsukuba, Tsukuba*  
<sup>52</sup>*Utkal University, Bhubaneswar*  
<sup>53</sup>*Virginia Polytechnic Institute and State University, Blacksburg, Virginia 24061*  
<sup>54</sup>*Yokkaichi University, Yokkaichi*  
<sup>55</sup>*Yonsei University, Seoul*

(Dated: December 3, 2018)

## Abstract

We report the observation of the decay  $D^0 \rightarrow \phi\gamma$  with a statistical significance of  $5.4\sigma$  in  $78.1 \text{ fb}^{-1}$  of data collected by the Belle experiment at the KEKB  $e^+e^-$  collider. This is the first observation of a flavor-changing radiative decay of a charmed meson. The Cabibbo- and color-suppressed decays  $D^0 \rightarrow \phi\pi^0$ ,  $\phi\eta$  are also observed for the first time. We measure branching fractions  $\mathcal{B}(D^0 \rightarrow \phi\gamma) = [2.60^{+0.70}_{-0.61} \text{ (stat.)}^{+0.15}_{-0.17} \text{ (syst.)}] \times 10^{-5}$ ,  $\mathcal{B}(D^0 \rightarrow \phi\pi^0) = [8.01 \pm 0.26 \text{ (stat.)} \pm 0.46 \text{ (syst.)}] \times 10^{-4}$ , and  $\mathcal{B}(D^0 \rightarrow \phi\eta) = [1.48 \pm 0.47 \text{ (stat.)} \pm 0.09 \text{ (syst.)}] \times 10^{-4}$ .

PACS numbers: 13.20.Fc, 14.40.Lb

Flavor changing radiative decays of the charmed meson system,  $D \rightarrow V\gamma$  where  $V$  is a vector meson, have not previously been observed. In the Standard Model, the short-distance contribution to these decays is negligible, and the contribution due to a vector meson coupling to a photon is expected to be dominant [1, 2]. For  $D^0 \rightarrow \phi\gamma$ , the branching fraction is expected to lie in the range  $(0.04 - 3.4) \times 10^{-5}$  [2, 3, 4]; the current 90% confidence level (C.L.) upper limit from CLEO is  $\mathcal{B}(D^0 \rightarrow \phi\gamma) < 1.9 \times 10^{-4}$  [5]. In the  $B$ -meson system, where the short-distance contribution to  $B \rightarrow X_d\gamma$  decay can be used to measure the CKM matrix element  $V_{td}$ , theoretical estimates of the long-distance contribution are also uncertain [6]. Measurement of radiative  $D$  meson decays therefore provides an important control on the interpretation of  $B \rightarrow X_d\gamma$  results.

In this paper, we present the first observation of the  $D^0 \rightarrow \phi\gamma$  decay. The analysis is based on  $78.1 \text{ fb}^{-1}$  of data collected at the  $\Upsilon(4S)$  resonance by the Belle detector [7] at the KEKB  $e^+e^-$  collider [8]. KEKB is a pair of electron storage rings with asymmetric energies, 3.5 GeV for  $e^+$  and 8 GeV for  $e^-$ , and a single interaction point. The Belle detector is a large-solid-angle general purpose spectrometer that consists of a three-layer silicon vertex detector (SVD), a 50-layer central drift chamber (CDC), an array of aerogel threshold Čerenkov counters (ACC), a barrel-like arrangement of time-of-flight scintillation counters (TOF), and an electromagnetic calorimeter comprised of CsI(Tl) crystals (ECL), located inside a superconducting solenoid coil that provides a 1.5 T magnetic field. An iron flux-return located outside of the coil is instrumented to detect  $K_L^0$  mesons and to identify muons (KLM).

According to a Monte Carlo (MC) study, the most important backgrounds to  $D^0 \rightarrow \phi\gamma$  are the Cabibbo- and color-suppressed decays  $D^0 \rightarrow \phi\pi^0$  and  $\phi\eta$ , which have not previously been observed either. We therefore conduct a search for these decay modes, and then optimise the selection criteria for  $D^0 \rightarrow \phi\gamma$  to take the contamination from  $\phi\pi^0$  and  $\phi\eta$  into account.

Common criteria are applied to select candidate events for various decay modes. Charged pions ( $\pi^\pm$ ) and kaons ( $K^\pm$ ) are reconstructed from tracks in the SVD and CDC which originate from the interaction region. Particle identification (ID) likelihoods for the pion ( $\mathcal{L}_\pi$ ) and kaon ( $\mathcal{L}_K$ ) hypotheses are determined from the ACC response, specific ionization ( $dE/dX$ ) measurement in the CDC and the time-of-flight measurement for each track. To identify kaons (pions), we apply a mode-dependent requirement on the likelihood ratio  $\mathcal{R} \equiv \mathcal{L}_K/(\mathcal{L}_K + \mathcal{L}_\pi)$ : a cut  $\mathcal{R} > 0.6$  ( $\mathcal{R} < 0.1$ ) yields an 86% (96%) efficiency for kaons (pions). We select  $\phi$  candidates from  $K^+K^-$  combinations in the invariant mass range  $1.01 < M_{K^+K^-} < 1.03 \text{ GeV}/c^2$ , and use combinations from the mass sidebands  $0.99 < M_{K^+K^-} < 1.00 \text{ GeV}/c^2$  and  $1.04 < M_{K^+K^-} < 1.05 \text{ GeV}/c^2$  to estimate the background under the  $\phi$  peak. The impact parameter cuts are also adopted for all charged particles,  $dr < 0.5 \text{ cm}$  and  $dz < 1.5 \text{ cm}$ , to suppress the background.

Neutral  $\pi$  mesons ( $\pi^0$ ) are formed from two photons, each with energy  $E_\gamma > 50 \text{ MeV}$ , and an invariant mass within  $\pm 16 \text{ MeV}/c^2$  ( $3\sigma$ ) of the nominal  $\pi^0$  mass; the photon momenta are then recalculated with a  $\pi^0$  mass constraint. For  $\eta \rightarrow \gamma\gamma$  reconstruction, we first combine each photon candidate ( $E_\gamma > 50 \text{ MeV}$ ) with every other photon ( $E_\gamma > 20 \text{ MeV}$ ) in the event: if the invariant mass of any combination is consistent with the  $\pi^0$  mass, we veto the photon candidate.  $\eta$  meson candidates are selected if the invariant mass of the photon pair is within  $\pm 40 \text{ MeV}/c^2$  ( $4\sigma$ ) of the  $\eta$  mass, and the photon momenta are then recalculated with an  $\eta$  mass constrained fit. Photons for  $D^0 \rightarrow \phi\gamma$  candidates are selected after applying the same  $\pi^0 \rightarrow \gamma\gamma$  veto described above.

$D^0$  candidates are formed from the combinations  $\phi\pi^0$ ,  $\phi\eta$  and  $\phi\gamma$  and then combined with  $\pi^+$  to form  $D^{*+}$  candidates for reduction of the combinatorial background. We calculate the difference in invariant mass,  $\Delta M = M_{D^0\pi^+} - M_{D^0}$ , and require  $138.6 < \Delta M < 142.6 \text{ MeV}/c^2$ .

Momentum cuts determined by maximizing  $N_{sig}/\sqrt{N_{bg}}$ , which is proportional to the expected significance of the signal, are applied for each mode; here  $N_{sig}$  is the number of selected signal events and  $N_{bg}$  is the number of selected background events in the MC. For  $D^0 \rightarrow \phi\gamma$ , the expected contamination from  $\phi\pi^0$  and  $\phi\eta$  is included as background. We select  $D^0 \rightarrow \phi\pi^0$  using a laboratory momentum cut of  $p_{\pi^0} > 750 \text{ MeV}/c$ ,  $D^0 \rightarrow \phi\eta$  using a cut  $p_\eta > 500 \text{ MeV}/c$ , and  $D^0 \rightarrow \phi\gamma$  by requiring  $E_\gamma > 450 \text{ MeV}$ . The  $D^*$  momentum in the center-of-mass is required to satisfy  $p_{D^*}^* > 2.9 \text{ GeV}/c$  for all modes; this cut is optimised for the selection of  $D^0 \rightarrow \phi\gamma$  and is above the kinematic limit for  $D^*$ 's produced in  $B$  decays at the  $\Upsilon(4S)$  resonance.

The reconstructed  $M_{\phi\pi^0}$  distribution shows a clear signal for  $D^0$  (Figure 1(a)). The distribution from non-resonant  $D^0 \rightarrow K^+K^-\pi^0$  decay also peaks at the  $D^0$  mass, and its contribution is evaluated and subtracted using the sideband of the  $M_{K^+K^-}$  distribution. The signal yield is extracted by fitting the sideband-subtracted  $M_{\phi\pi^0}$  distribution in the range  $[1.72 - 1.95] \text{ GeV}/c^2$  assuming an exponential shape for the background and a signal shape developed by the Crystal Ball experiment [9]. From the  $\chi^2$  fitting, we obtain  $1254 \pm 39$  events. Due to the conservation of angular momentum the distribution in helicity angle  $\theta_{hel}$ , the angle between the  $K^+$  momentum direction and the  $D^0$  momentum direction in

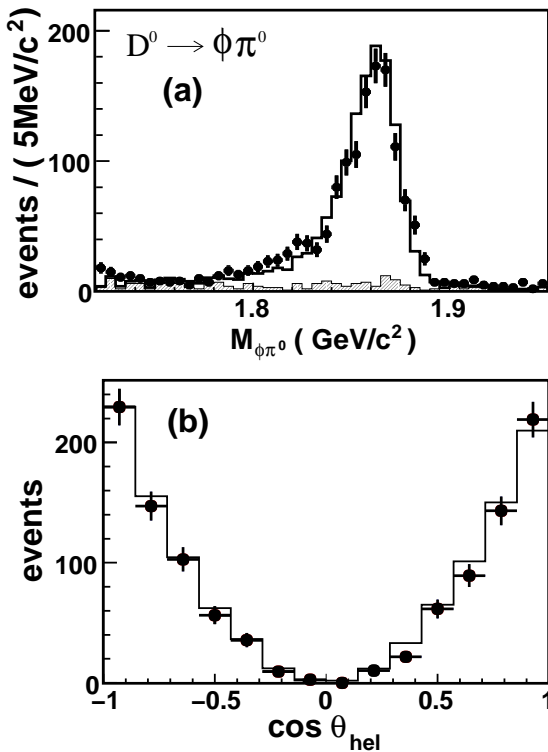


FIG. 1:  $D^0 \rightarrow \phi\pi^0$ : (a) invariant mass distribution for data (points with errors),  $\phi\pi^0$  combinations from the  $\phi$ -mass sideband in  $M_{K^+K^-}$  (shaded histogram), and sideband + signal (open histogram); (b) fitted  $D$  yield in bins of  $\cos \theta_{hel}$  (points with errors) ( $\theta_{hel}$  is the  $\phi$  helicity angle) and the MC prediction (histogram).

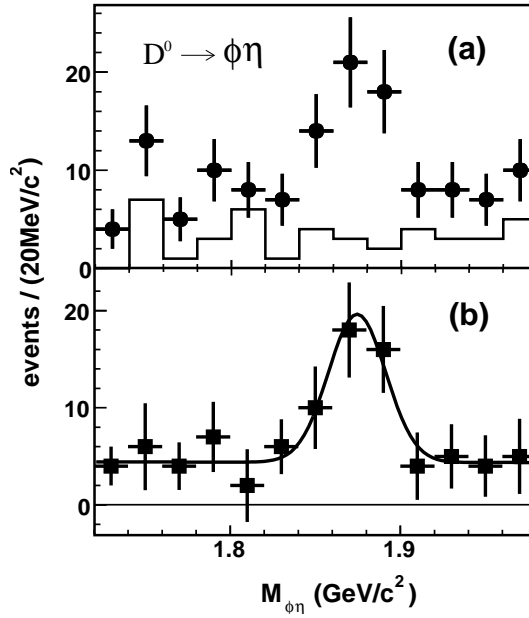


FIG. 2:  $D^0 \rightarrow \phi\eta$ : (a) invariant mass distribution for data (points with errors) and the  $\phi$ -mass sideband (histogram); (b) background-subtracted distribution, with a fit function described in the text (solid curve).

the rest frame of the  $\phi$  meson, is expected to be proportional to  $\cos^2 \theta_{hel}$  for  $D^0 \rightarrow \phi\pi^0$  and  $\phi\eta$  decays but proportional to  $\sin^2 \theta_{hel}$  for  $D^0 \rightarrow \phi\gamma$ . The distribution in  $\cos \theta_{hel}$  for the  $D^0 \rightarrow \phi\pi^0$  candidates is consistent with  $\cos^2 \theta_{hel}$ , as shown in Figure 1(b). The background to  $D^0 \rightarrow \phi\gamma$  from  $\phi\pi^0/\phi\eta$  decay is thus strongly suppressed by a requirement on  $\theta_{hel}$ .

The  $M_{\phi\eta}$  distribution and the contribution from the  $M_{K^+K^-}$  sideband are shown in Figure 2(a). We extract the signal yield from the sideband-subtracted  $M_{\phi\eta}$  distribution shown in Figure 2(b). The  $\chi^2$  fit yields  $31.1 \pm 9.8$  signal events, where Gaussian and first-order polynomial shapes are assumed for the signal and background, respectively.

For the radiative mode, we require  $E_\gamma > 450$  MeV and  $\cos \theta_{hel} < 0.4$  based on optimization of  $N_{sig}/\sqrt{N_{bg}^{\phi\pi^0} + N_{bg}^{\phi\eta} + N_{bg}^{others}}$ , where  $N_{bg}^{\phi\pi^0}$  and  $N_{bg}^{\phi\eta}$  are scaled to be consistent with the observed signals in those modes. A clear signal is observed in the  $M_{\phi\gamma}$  invariant mass distribution (Figure 3(a)). The signal yield is extracted using the binned maximum likelihood method. The shapes of signal and feeddown background from  $D^0 \rightarrow \phi\pi^0$ ,  $\phi\eta$  and  $D^+ \rightarrow \phi\pi^+\pi^0$  are obtained by MC simulation. The normalizations of the feeddown backgrounds are fixed based on the rates observed in the signal analyses described earlier, and their uncertainties are assigned as the systematic error. The shape of the combinatorial background is estimated by selecting entries from the sideband of the  $M_{K^+K^-}$  distribution and fitting to a first-order polynomial shape. The normalization of this contribution is floated in the fit. The extracted yield is  $27.6^{+7.4}_{-6.5}$  (stat.)  $^{+0.5}_{-1.0}$  (syst.) events. The significance of the signal, taken to be  $\sqrt{-2 \ln (L_0/L_{best})}$  where  $L_{best}$  and  $L_0$  are the maximum likelihood values with the signal floated and fixed to zero, respectively, is  $5.4\sigma$ .

The fitting procedure is checked by comparing the yields from fitting and from counting with background subtraction. The signal yield from the counting method is  $28.2 \pm 9.8$  (stat.)  $\pm 3.7$  (syst.). If the signal region is limited to  $[1.78 - 1.92] \text{ GeV}/c^2$ , the signal

yield from counting is  $29.1 \pm 7.0$  (stat.)  $\pm 0.5$  (syst.), and the fitted signal yield within the restricted region is  $26.6^{+7.1}_{-6.4}$  (stat.)  $^{+0.5}_{-1.0}$  (syst.). In both cases, the results are consistent.

With the signal region defined as  $[1.78-1.92] \text{ GeV}/c^2$ , an excess of signal over background is observed near  $\cos \theta_{hel} \sim 0$  (Figure 3(b)). The feeddown from  $D^0 \rightarrow \phi \pi^0$  and  $\phi \eta$  is larger with a looser helicity cut. Figure 3(c) shows the helicity angle distribution after background subtraction. It is consistent with the  $\sin^2 \theta_{hel}$  distribution expected for the  $D^0 \rightarrow \phi \gamma$  signal.

To minimize systematic uncertainties, we measure the branching fraction as a ratio to  $D^0 \rightarrow K^+ K^-$ , where we have a signal of  $21787 \pm 226$  events, and derive the branching fraction using the world average  $\mathcal{B}(D^0 \rightarrow K^+ K^-)$  [10]. Many of the systematic errors associated with tracking and particle ID are at least partially canceled in the ratio.

The reconstruction efficiencies are estimated via MC simulation. Some differences in efficiency between data and MC have been noted, in particular for photon and  $\pi^0$  reconstruction. The difference in the  $\pi^0$  efficiency is studied using the double ratio of the two decay modes of  $\eta$ ,

$$\frac{\varepsilon_{data}(2\pi^0)}{\varepsilon_{MC}(2\pi^0)} = \frac{N_{data}(\eta \rightarrow 3\pi^0)/N_{MC}(\eta \rightarrow 3\pi^0)}{N_{data}(\eta \rightarrow \gamma\gamma)/N_{MC}(\eta \rightarrow \gamma\gamma)},$$

where  $[\varepsilon_{data}(\pi^0 \rightarrow \gamma\gamma)/\varepsilon_{MC}(\pi^0 \rightarrow \gamma\gamma)]_{\eta \rightarrow 3\pi^0} = \varepsilon_{data}(\eta \rightarrow \gamma\gamma)/\varepsilon_{MC}(\eta \rightarrow \gamma\gamma)$  is assumed.

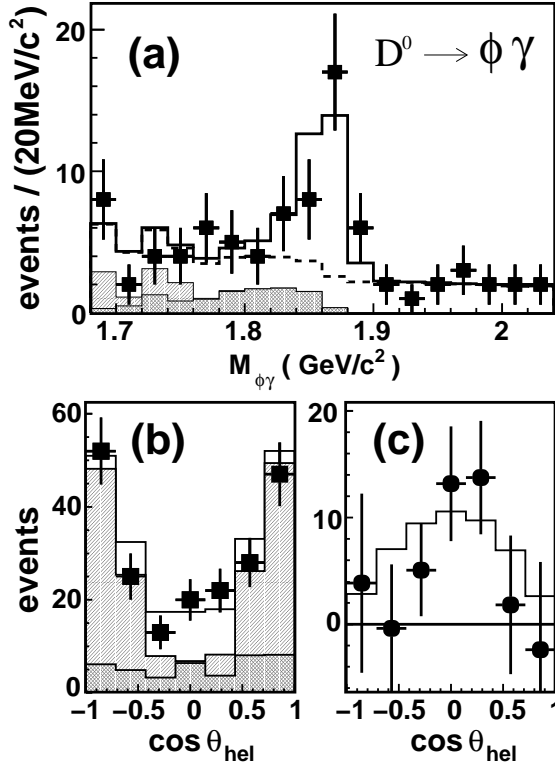


FIG. 3:  $D^0 \rightarrow \phi \gamma$ : (a) invariant mass distribution for data (points with errors), the fit described in the text (open histogram), the background component of the fit (dashed),  $\phi \pi^0$  background (dark histogram), and the sum of  $\phi \eta$ , and  $D^+ \rightarrow \phi \pi^+ \pi^0$  backgrounds (light); (b)  $\cos \theta_{hel}$  distribution in the signal region, with the MC predictions: total (open), total background (light), and non- $\phi \pi^0$  background (dark histogram); (c) background-subtracted  $\cos \theta_{hel}$  distribution and the MC prediction (histogram).

The efficiency correction factors estimated from this study are found to be  $(97.90 \pm 2.70)\%$  for  $\pi^0$  ( $E_\gamma > 50$  MeV and  $P_{\pi^0} > 750$  MeV/c),  $(96.20 \pm 1.56)\%$  for  $\eta$  ( $E_\gamma > 50$  MeV and  $P_\eta > 500$  MeV/c) and  $(98.5 \pm 1.91)\%$  for a signal  $\gamma$  with  $E_\gamma > 450$  MeV (assuming  $\varepsilon_{\pi^0} = \varepsilon_\gamma \times \varepsilon_\gamma$ ). The overall detection efficiencies are summarized in Table I.

The systematic uncertainties are summarized in Table II. The errors derived from the fitting process and background contribution are estimated by changing the fitting range, bin width, and background contributions by the amount of the uncertainties. The uncertainty in the acceptance due to the  $m_{K^+K^-}$  requirement for  $\phi$  candidates is estimated by changing the ratio  $R_{D^0 \rightarrow \phi\pi^0} \equiv [N_{data}/N_{MC}]_{D^0 \rightarrow \phi\pi^0}$  while shifting the signal region by  $\pm 1$  MeV/c<sup>2</sup>. Other systematic errors are estimated by observing changes to the double ratio,  $R_{D^0 \rightarrow \phi\pi^0}/R_{D^0 \rightarrow K^+K^-}$ . The error in tracking efficiency is estimated by changing the impact parameter criteria;  $dr < 0.5 \rightarrow 0.3$  cm and  $dz < 1.5 \rightarrow 1.0$  cm. We applied the same method to estimate the systematic errors from particle ID and mass difference ( $\Delta M$ ) criteria;  $\mathcal{R} > 0.6 \rightarrow 0.5$  for kaons,  $\mathcal{R} < 0.1 \rightarrow 0.5$  for pions and  $\Delta M \rightarrow \Delta M \pm 1$  MeV/c<sup>2</sup>. Due to the difference in the momentum distribution of  $K^\pm$  between the  $\phi\pi^0$  and  $K^+K^-$  modes, the uncertainty on the particle ID efficiency does not cancel in the ratio. The uncertainties in the branching fractions of submodes are taken from the current world averages [10].

TABLE I: Detection efficiencies for various  $D^0$  decay modes [%]

Mode ( $D^0 \rightarrow$ )	$K^+K^-$	$\phi\pi^0$	$\phi\eta$	$\phi\gamma$
Reconstruction	10.4	6.48	0.87	4.32
	$\pm 0.1$	$\pm 0.04$	$\pm 0.02$	$\pm 0.04$
$\mathcal{B}(\phi \rightarrow K^+K^-)$	—	49.20	49.20	49.20
$\mathcal{B}(\pi^0 \rightarrow 2\gamma)$	—	98.80	—	—
Efficiency correction	—	97.90	96.20	98.50
for $\pi^0 / \eta / \gamma$				
Total	10.40	3.08	0.413	2.09

TABLE II: Estimated systematic errors [%]

	$D^0 \rightarrow \phi\pi^0$	$D^0 \rightarrow \phi\eta$	$D^0 \rightarrow \phi\gamma$
Tracking etc.	0.59	0.59	0.59
Particle ID	2.74	2.74	2.74
$\Delta M$	0.98	0.98	0.98
Mass of $\phi$	0.94	0.94	0.94
Efficiency correction	2.75	1.62	1.94
for $\pi^0/\eta/\gamma$			
Fitting & BG	0.99	1.48	+2.06/-3.75
$\mathcal{B}(D^0 \rightarrow K^+K^-)$	3.40	3.40	3.40
$\mathcal{B}(\phi \rightarrow K^+K^-)$	1.42	1.42	1.42
$\mathcal{B}(\pi^0/\eta \rightarrow 2\gamma)$	0.03	0.66	—
MC statistics	0.99	2.76	1.11
Total	5.73	6.01	+5.70/-6.50

To summarize, we have observed the decay  $D^0 \rightarrow \phi\gamma$  for the first time. Its branching fraction is

$$\mathcal{B}(D^0 \rightarrow \phi\gamma) = [2.60^{+0.70}_{-0.61} (\text{stat.}) \pm 0.15 (\text{syst.})] \times 10^{-5}.$$

We also observe two other rare decays. These modes are Cabibbo-suppressed and color-suppressed, and constitute backgrounds for the radiative mode. Their branching fractions are

$$\begin{aligned}\mathcal{B}(D^0 \rightarrow \phi\pi^0) &= [8.01 \pm 0.26 (\text{stat.}) \pm 0.46 (\text{syst.})] \times 10^{-4}, \\ \mathcal{B}(D^0 \rightarrow \phi\eta) &= [1.48 \pm 0.47 (\text{stat.}) \pm 0.09 (\text{syst.})] \times 10^{-4}.\end{aligned}$$

The radiative  $D \rightarrow V\gamma$  decays are expected to be dominated by long-distance contributions, however, the theoretical uncertainty on the rate is very large (2-3 orders of magnitude). Short-distance contributions are important only if the long-distance contribution is suppressed, in which case the branching fraction is predicted to be less than  $10^{-8}$ , even for Cabibbo-favored modes. Thus, this observation of  $D^0 \rightarrow \phi\gamma$  constitutes evidence for significant long-distance contributions, and it provides an anchor for the further development of non-perturbative QCD.

We wish to thank the KEKB accelerator group for the excellent operation of the KEKB accelerator. We acknowledge support from the Ministry of Education, Culture, Sports, Science, and Technology of Japan and the Japan Society for the Promotion of Science; the Australian Research Council and the Australian Department of Education, Science and Training; the National Science Foundation of China under contract No. 10175071; the Department of Science and Technology of India; the BK21 program of the Ministry of Education of Korea and the CHEP SRC program of the Korea Science and Engineering Foundation; the Polish State Committee for Scientific Research under contract No. 2P03B 01324; the Ministry of Science and Technology of the Russian Federation; the Ministry of Education, Science and Sport of the Republic of Slovenia; the National Science Council and the Ministry of Education of Taiwan; and the U.S. Department of Energy.

---

[1] B.Bajc et al., Phys. Rev. D **51**, 2230 (1995).  
[2] G. Burdman et al., Phys. Rev. D **52**, 6383 (1995).  
[3] S. Fajfer et al., Phys. Rev. D **56**, 4302 (1997).  
[4] S. Fajfer et al., The Eur. Phys. Jour. C **6**, 471 (1999).  
[5] D.M. Asner et al., (CLEO Collaboration), Phys. Rev. D **58**, 092001 (1998).  
[6] A. Khodjamirian et al., Phys. Lett. B **358**, 129 (1995), H.Y. Cheng, Phys. Rev. D **51**, 6228 (1995), A. Ali and V.M. Braun, Phys. Lett. B **359**, 223 (1995), J.F. Donoghue et al., Phys. Rev. D **55**, 2657 (1997).  
[7] A. Abashian et al. (Belle Collaboration), Nucl. Instr. Meth. A **479**, 117 (2002).  
[8] S. Kurokawa and E. Kikutani, Nucl. Instrum. Meth., A **499**, 1 (2003), and other papers included in this Volume.  
[9] T. Skwarnicki, Ph.D. Thesis, Institute for Nuclear Physics, Krakow 1986; DESY Internal Report, DESY F31-86-02 (1986).  
[10] K. Hagiwara et al., Phys. Rev. D **66**, 010001 (2002).